HEAT 2008, Fifth International Conference on
Transport Phenomena In Multiphase Systems
June 30 - July 3, 2008, Bialystok, Poland

A Computational Study of Cavitation in a Hydraulic Poppet Valve

Mohammad Passandideh-Fard[1] and Hossein Moin[2]

[1]Assistant Professor, Ferdowsi University of Mashhad, Iran (mpfard@um.ac.ir)
[2]Graduate Student, Ferdowsi University of Mashhad, Iran (h.moin.jnr@gmail.com)

Abstract

Transient incipient cavitation in an oil hydraulic poppet valve is numerically simulated using a computational model based on Volume-of-Fluid (VOF) technique where transient 2D/axisymmetric Navier-Stokes equations are solved along with an equation to track the cavity interface. The numerical results are compared with those of the available experiments in the literature. The method is then used to improve the hydraulic valve performance based on cavitation regimes in flow separation point. The effects of the poppet angle (at a constant poppet base and displacement) are discussed.

Keywords: *cavitation, poppet valve, hydraulic valve, volume of fluid, two phase flow*

INTRODUCTION

In this study, the flow cavitation in a poppet valve, which is a typical hydraulic element in fluid power engineering systems, is numerically simulated. Poppet valves as the industrial directional control valves are characterized by having a movable element (the poppet) to direct the flow through the valve body. From the controlling flow of rocket fuel to controlling the car wash equipment, poppet valves are used in many industrial processes.

Cavitation is a common phenomenon in many flow instruments such as valves, compressors, pumps and also piping systems. Cavitation in water flows has been studied by many researchers for well over 100 years. This phenomenon, however, may occur in other liquids such as oil even though it has been rarely investigated in the literature. Cavitation is commonly classified by a cavitation number:

$$\sigma = \frac{(P_\infty - P_v)}{(\frac{1}{2}\rho V_\infty^2)} \quad (1)$$

where P_v is the vapor pressure, ρ the liquid density, and P_∞, V_∞ are the main flow pressure and velocity, respectively. For non-aqua liquids, a second definition of cavitation number has also been introduced as (Takahashi et al., 2003):

$$\sigma = \frac{P_D}{(P_U - P_D)} \quad (2)$$

where P_D and P_U are the pressures downstream and upstream of the flow, respectively. Complex characteristics of cavitating flows such as sharp changes in the fluid density, existence of a moving boundary and the requirement of modeling phase change prevented the development of computational algorithms based on Navier-Stokes equations. Following the advancement in CFD methods, cavitation models based on Navier-Stokes equations emerged in early 1990's. These models are divided into two main categories: interface tracking method and homogeneous equilibrium flow (Passandideh-Fard and Roohi, 2008). In interface tracking method, a constant pressure (vapor pressure) is assumed inside the cavity and a wake model is used to predict the shape of the cavity interface in adaptive grids. In the second category, used in this study, the density field is estimated by various models from which the method based on single-fluid modeling has been shown to be more accurate (Passandideh-Fard and Roohi, 2008). In this approach, an advection equation for liquid (or vapor) volume fraction is solved and the density is computed according to the volume fraction of the two phases. This approach, so-called Transport based Equation Model (TEM), has been widely applied to simulate cavitation. The selection of an appropriate mass transfer model and an algorithm for advection equation are the main issues. Yuan et al. (2001) suggested a cavitation model based on Rayleigh relation. Singhal et al. (2002), Merkle et al. (1998) and Kunz et al. (2000) have used different mass transfer models based on semi-analytical equations.

A well-known method to solve the advection of a free-surface such as a cavity interface is VOF technique. Frobenius and Schilling (2003) and Wiesche (2005) used this technique to simulate cavitation over hydrofoils and pump impellers. A review of the reported literature reveals that VOF method can accurately capture cavity shape and characteristics. In this study, a modified VOF technique based on Youngs' PLIC algorithm (Youngs, 1982) is combined with a mass transfer model of Kunz et al. (2000) to simulate cavitation.

Although cavitation phenomenon can occur in all liquid flows, water flow cavitation has received more attention in the literature. Very recently other types of liquid flows were investigated in cavitation studies. Unsteady cavitation of liquid hydrogen in an orifice and that of oxygen in a turning duct venturi were simulated by Ahuja and Hosangadi (2006). Dumont et al. (2001) also studied the cavitation in diesel injectors using a homogenous equilibrium modeling approach. Another cavity simulation of an automotive fuel jet pump was performed by Wiesche (2005) who employed the VOF method with k-ε turbulence model to solve the Navier-Stokes equations. Early experiments on cavitation in hydraulic oil

date back to 1994. Oil cavitation in a complex geometry of a poppet valve was studied by Washio et al. (2006).

In this study, the incipient cavitation for an oil hydraulic flow in a poppet valve with an axisymmetric configuration is simulated. Numerical results are compared with those of the available experiments where the two results for flow behavior are discussed on differences and similarities. The effects of the poppet angle (at a constant poppet base and displacement) are then investigated in order to improve the valve performance with regard to the reduction of cavitation.

NUMERICAL METHOD

In this study, the advection of the cavity interface is simulated based on Volume-of-Fluid (VOF) technique along with a cavitation model for mass transfer between the two phases of liquid and vapor.

Volume-of-Fluid (VOF) Algorithm

The governing equations for the 2D/axisymmetic incompressible fluid flow are

$$\vec{\nabla}.\vec{V} = 0 \tag{3}$$

$$\frac{\partial \vec{V}}{\partial t} + \vec{\nabla}.(\vec{V}\vec{V}) = -\frac{1}{\rho}\vec{\nabla}P + \frac{1}{\rho}\vec{\nabla}.\vec{\tau} + \frac{1}{\rho}\vec{F}_b + \vec{g} \tag{4}$$

where $\vec{V}$ is the velocity vector, P indicates the pressure, $\vec{F}_b$ represents body forces acting on the fluid, $\vec{g}$ is the acceleration due to gravity and $\vec{\tau}$ represents the viscous stress tensor. The phase change boundary is defined by Volume-of-Fluid (VOF) method where a scalar field is defined whose value is equal to zero in the vapor phase and one in the liquid. When a cell is partially filled with liquid, f has a value between zero and one. The discontinuity in f is propagating through computational domain according to:

$$\frac{df}{dt} = \frac{\partial f}{\partial t} + \vec{V}.\vec{\nabla}f = S \tag{5}$$

where S is the appropriate cavitation mass transfer sink term. This equation with appropriate mass transfer models can be used to simulate many physical phenomena such as cavitation, vaporization and condensation. The Hirt-Nichols (1981) and Youngs PLIC (1982) methods are widely used for the advection of the volume of fraction f in Eq. 5. Although the Hirt-Nichols has been used in most cavity simulations, in this study the Youngs method which is more accurate is employed. To begin the advection using Eq. 5, an intermediate value of f is introduced as:

$$\tilde{f} = f^n - \delta t\,\vec{\nabla}.(\vec{V}f^n) \tag{6}$$

and "divergence correction" completes the scheme:

$$f^{n+1} = \tilde{f} + \delta t(\vec{\nabla}.\vec{V})f^n + \delta t(S^n) \tag{7}$$

This scheme initiates the distribution of f for velocity and pressure calculations in each time step. Because a single set of equations is solved for both phases, mixture properties are used as:

$$\begin{aligned} \rho &= f\rho_l + (1-f)\rho_v \\ \mu &= f\mu_l + (1-f)\mu_v \end{aligned} \tag{8}$$

where subscripts l and v denote the liquid and vapor, respectively. Two-step time projection method is employed for the solution of momentum equation. First an intermediate velocity is calculated based on the terms related to advection, viscosity and body forces:

$$\frac{\tilde{\vec{V}} - \vec{V}^n}{\delta t} = -\vec{\nabla}(\vec{V}\vec{V})^n + \frac{1}{\rho^n}\vec{\nabla}.\vec{\tau} + \vec{g}^n + \frac{1}{\rho^n}\vec{F}_b^n \tag{9}$$

Continuum Surface Force (CSF) method (Brackbill et al., 1992) is used to treat the surface tension in interfacial cells as a body force. Pressure field obtained by Poisson equation:

$$\vec{\nabla}.(\frac{1}{\rho}\vec{\nabla}P^{n+1}) = \frac{\vec{\nabla}.\tilde{\vec{V}}}{\delta t} \tag{10}$$

An Incomplete Cholesky Conjugate Gradient Decomposition (ICCG) solver is employed for solving this equation. Having calculated the new time level pressures, the velocities are updated using:

$$\frac{\vec{V}^{n+1} - \tilde{\vec{V}}}{\delta t} = -\frac{1}{\rho}\vec{\nabla}P^{n+1} \tag{11}$$

Cavitation Model

Several cavitation mass transfer models can be used to replace S in Eq. 5. Among the more recommended models we have the Rayleigh equation and semi-analytical schemes (Passandideh-Fard and Roohi, 2008). Many semi-analytical schemes are based on the modified Rayleigh theory or a mass-momentum interaction model around the cavity interface (Passandideh-Fard and Roohi, 2008, and Bussmann et al. 1999). In current study, the semi-analytical model of Kunz is used to treat S in Eq. 5:

$$\begin{aligned} \frac{\partial f}{\partial t} + \vec{V}.\vec{\nabla}f = {} & \frac{C_{dest}\rho_l Min(P_l - P_v, 0)f}{(\tfrac{1}{2}\rho_l V_\infty^2)\rho_v t_\infty} \\ & + \frac{C_{prod}(1-f)f^2}{\rho_l t_\infty} \end{aligned} \tag{12}$$

where $C_{dest} = 9\times10^5$ and $C_{prod} = 3\times10^4$ are numerical-experimental weighting coefficients offered by Kunz et al. (2000) which are calculated based on the Rayleigh analytical equation and the related experimental measurements. Flow characteristic time, t_∞, is defined as the ratio of the maximum solid-body diameter to the main flow velocity. As seen from Eq. 12, no temperature terms exists in the cavitaion model because the effect of viscous dissipation on fluid temperature is negligible. As a result, in most cavitation studies available in the literature, the flow was assumed isothermal. The advection equation for liquid volume fraction (Eq. 6) is solved using a modified VOF method based on Youngs' PLIC algorithm (Bussmann et al., 1999) combined with a mass transfer model of Kunz et al. (2000). The density field is then calculated based on the volume fraction of each phase in a computational cell. Details of the numerical model are given elsewhere (Passandideh-Fard and Roohi, 2008, and Bussmann et al., 1999) and will not be repeated here.

RESULTS and DISCUSSION

In this section, first we present a comparison between numerical results with those of the available experiments to validate the simulations. The model is then used to investigate different poppet valve characteristics in order to improve its performance based on cavitation phenomenon.

Model Validation

The method described above is used to simulate the cavity formation in a poppet valve seat for a case for which experimental photographs are available (Kikui et al., 2006). A schematic of the valve under consideration is shown in Fig. 1. All simulations are performed for ISO-VG46 machine oil, a liquid commonly used in industrial hydraulic systems, with properties given as 73×10^{-6} m^2/s for the kinematic viscosity, and 900 kg/m^3 for the density at a temperature of 30°C (Takahashi et al., 2003). The computational domain selected for this simulation was 15 mm×12 mm with a mesh resolution that had 10 cells per one millimeter. This mesh resolution was set based on a mesh refinement study, and is used for the entire simulations in this paper.

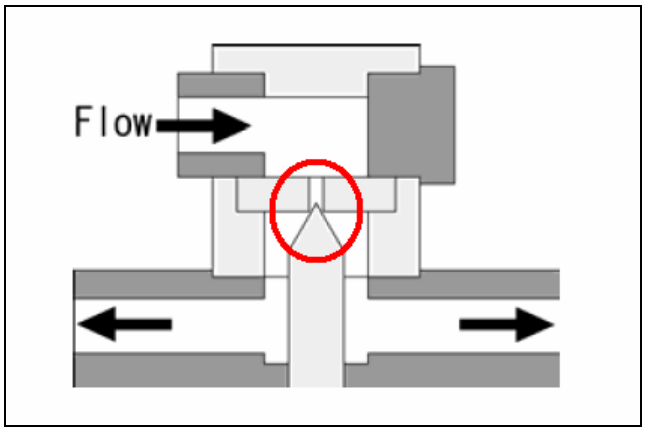

Fig. 1. Schematic of a poppet valve (Kikui et al., 2006). The section under consideration is the region inside the circle shown.

Figure 2 compares the cavitation formation observed in experiments and predicted by the model. As shown in the figure, cavitation starts as a sudden appearance of a small perturbation (bubble) on the edge of the valve seat where the flow separation occurs. This phenomenon is seen 6.7 ms after the start of the flow into the valve for conditions that the poppet displacement was 0.5 mm and the flow rate was increased linearly from 2 to 40 cm^3/s in 66.7 ms.

A reduced pressure region close to the valve seat, seen from the simulations (Fig. 2, 6.7 ms), indicates the location where the cavitation will occur. Since the model is 2D/axisymmetric, it does not predict the transient characteristics of cavitation inception. However, when pressure all around the separation zone decreased below that of the vapor pressure, a full cavity region was formed. Therefore, the use of the model in this condition is justified. At 66.7 ms elapsed from the oil flow into the valve, both the experiment and the model predict a cavity all around the valve seat, thereby, causing a serious failure in its performance. This instance is also shown in Fig. 2 where the cavity is indicated as a black region in the photograph (due to light deflection at the cavity interface) and a vapor region in the numerical image. Pressure distributions and flow streamlines are also shown in the numerical images of Fig. 2. In the cavity region, the pressure is reduced to that of the vapor pressure and the flow streamlines are disturbed as seen in the figure.

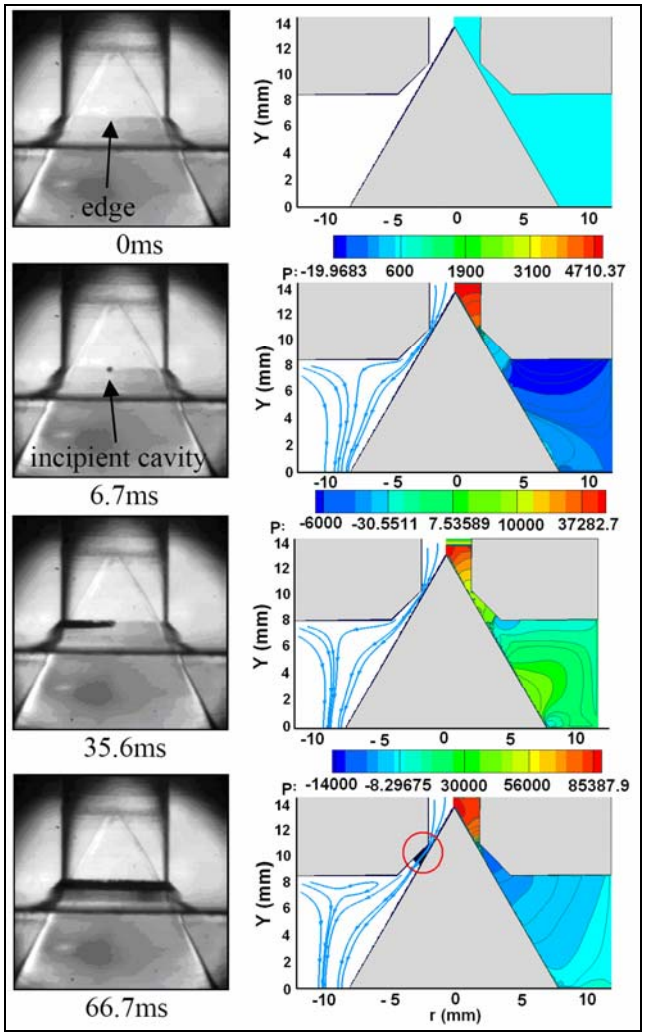

Fig. 2. Inception of cavitation from experiment (Kikui et al., 2006) and numerical model. The pressure distribution and flow streamlines are also seen in the numerical image.

Figure 3 shows a close-up view of the separation point where cavitation starts. The pressure distribution along with flow streamlines and velocity vectors are displayed in the figure. The images shown in this figure correspond to the transient fluid flow; as a result, the pressure changes from one time to the next are significant. Therefore, the pressure contour levels in each image of Fig. 3 are different. The minimum pressure at the beginning of the flow (6.7 ms) is observed at the end of the valve channel. As time passes, the absolute value of the minimum pressure is decreased and its

location is gradually nearing the poppet minimum cross-sectional area. When cavitation occurs, the value of the minimum pressure falls below that of the vapor pressure and its location is fixed at the valve minimum cross-sectional area. The velocity distribution is also shown in the figure. As seen, the velocity profile before the separation point is parabolic; after this point, however, the flow recirculation occurs.

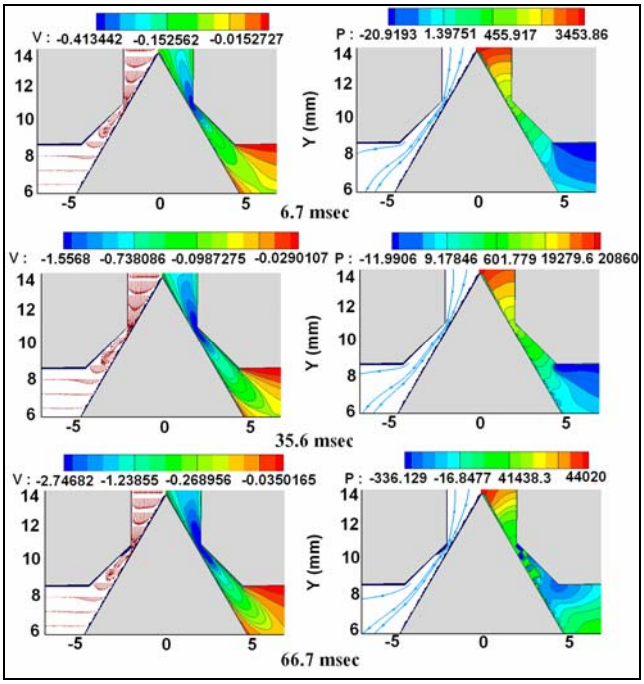

Fig. 3. Close-up view of separation point in the poppet valve. The left side shows velocity distribution and contours; and the right side pressure distribution and streamlines.

When a cavity region is formed, the pressure distribution experiences a sudden change. The cavity is; therefore, detached from the solid surface and is driven downstream by the liquid flow. The next cavity will then be formed at the valve seat and the entire process will be repeated. Figure 4 shows the results of simulation and experiment for a case with a flow rate of 119 cm^3/s through the valve. A semi-steady cavitation is formed in this case as seen in both photograph and calculated image. This phenomenon is seen as pressure fluctuations in the valve as shown in Fig. 5 from both measurements and numerical model. The numerical points for pressure fluctuations in Fig. 5 are only given at time steps used in the simulation. The cavity in this case never comes to a steady shape and the pressure oscillates intermittently. While the mean pressure fluctuations are well predicted by the axisymmetric model, the instantaneous fluctuations being a transient 3D phenomenon were not captured.

Effects of Important Parameters

In this section, the effects of important valve geometric parameters on its performance are discussed. One aspect of a poppet valve design is based on the effects of these parameters

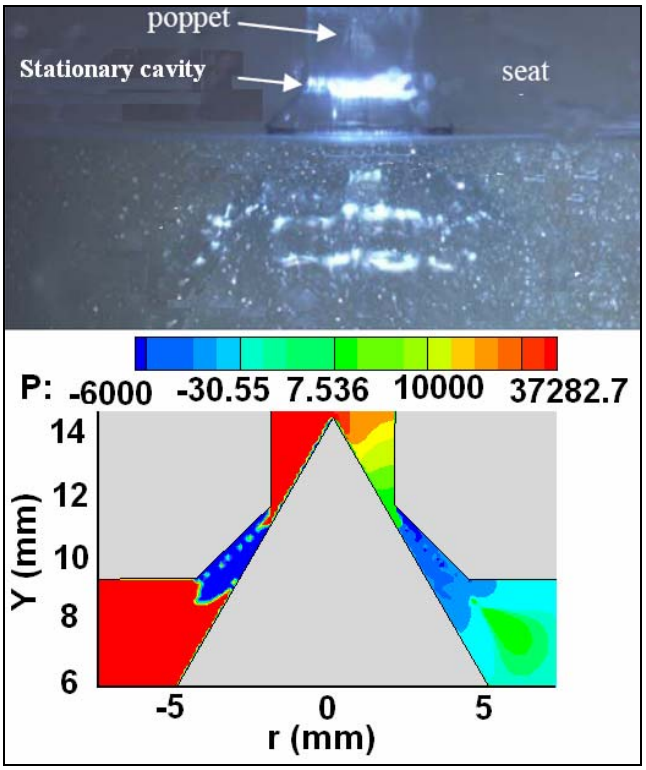

Fig. 4. An experimental photograph (Kikui et al., 2006) and a numerical image of the cavity formation in the poppet valve with a flow rate of 119 cm^3/s.

on the cavitation formation. A design with less cavitation is more favorable. The parameters considered here are the poppet angle and the poppet height. To characterize the flow cavitation in the valve we define a dimensionless number as

$$\xi = \frac{A^*}{A} \tag{13}$$

where A is the minimum cross-sectional flow area around the poppet and A^* is the liquid passing area with no cavitation. The parameter, therefore, indicates the fraction of the minimum area with no cavitation. For the cases studied here the radius of the poppet base and the axial displacement of the poppet were considered constant with values of r=8 mm and x=0.5 mm, respectively. The poppet height, therefore, is related to the poppet angle. We considered five cases with poppet angles ranging from 45° to 115°. The flow rate for all cases was considered to increase linearly from 2 to 40 cm^3/s in 66.7 ms. With this flow rate, even at the maximum value of 40 cm^3/s, the Reynolds number at the valve entrance is less than 175 and at minimum cross-sectional area is less than 350. As a result, turbulence effects are not important and the fluid flow can be considered laminar.

Figure 6 shows the pressure contour, flow streamlines and velocity distribution for a poppet valve with an angle of 45°. In this case, the cavitation occurs at 35.6 ms elapsed from the start of the oil flow into the valve. Compared to the case with a poppet angle of 60° (Fig. 3), the cavitation occurs in a faster time because the outflow from the valve exits in a channel with a wider diverging angle. The evolution of the cavity growth with time is also seen in Fig. 6.

The numerical results for a poppet valve with an angle of

75° are displayed in Fig 7. Compared to the previous cases with 45° (Fig. 6) and 60° angles (Fig. 3), the cavitation time is delayed. In this case, after 60.3 ms from the start of the flow, a full cavitation is seen at the minimum cross-sectional area of the valve. For all these cases, the valve exit channel has a diverging configuration. The next case considered is that of a valve with an angle of 90° for which the inner and outer surfaces of the channel are parallel. Figure 8 shows the simulation results for this case. As seen, the fluid in this case remains as liquid and no cavitaion is occurring. In contrast to the previous cases, flow vortices are not observed, the pressure distribution is continuous, and the location of the minimum pressure is at the end of the valve seat. As a result, a poppet angle of 90° seems to be a better design for the valve because it prevents the cavity formation. However, this angle causes an operational problem in the valve performance and, therefore, is not used practically. When the valve is closing, because the inner and outer surfaces of the exit channel are parallel, the two surfaces completely cover one another. As a result, the valve cannot be opened easily.

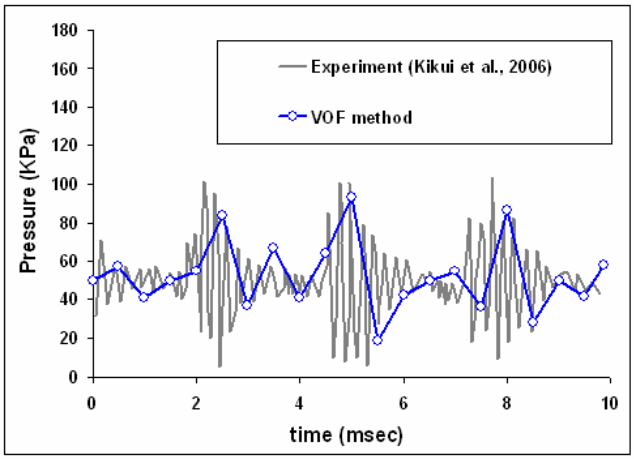

Fig. 5. Downstream pressure fluctuations in the valve due to cavitation from experiments (Kikui et al., 2006) and numerical model. The flow rate through the valve was 119 cm^3/s in this case.

To complete the poppet angle effect, we consider one final case for which the angle is 115°. In this case, the conical flow channel is converging. Figure 9 shows the results for this poppet angle. As seen from the figure, cavitation does not occur in the valve. For this case, the operational problem of the valve with 90° does not exit either; as a result, this design appears to be more favorable.

To compare the effects of valve angle more clearly, the thrust force under the poppet vs. time for all cases are shown in Fig. 10. As the inflow to the channel is increasing with time, this figure displays the effect of inflow variation on the thrust force as well. The force versus time (or channel inflow) appears to be a semi-linear curve in all poppet angles. As observed, the thrust force for a valve with a higher angle is increased. When the poppet angle is 90°, the thrust force has the maximum value because of the shear stresses between two parallel surfaces are higher than those of a diverging or converging channel.

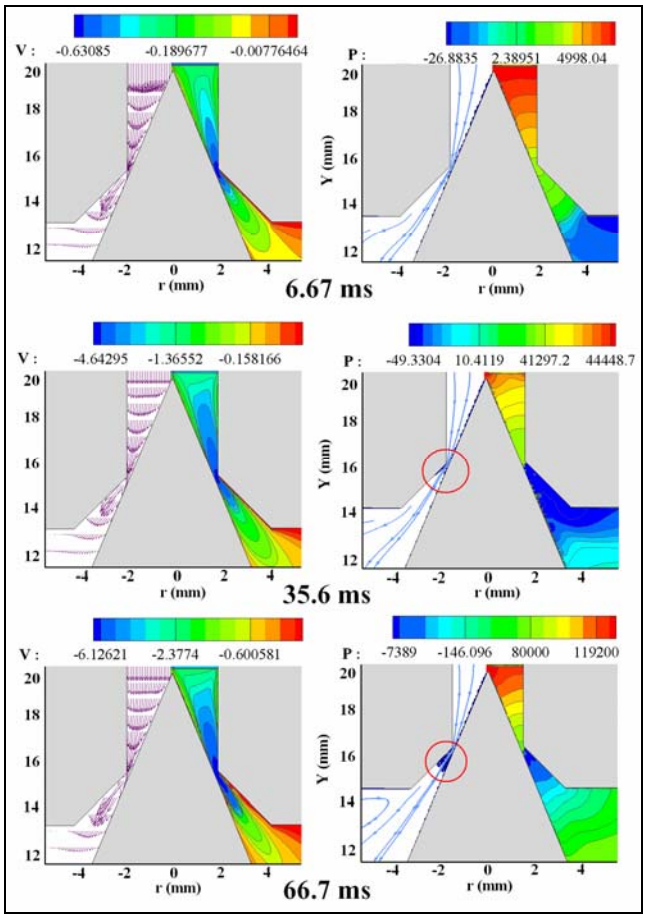

Fig. 6. Cavity formation (shown with a circle) in a poppet valve with 45° angle. Left: velocity distribution and contours. Right: pressure distribution and flow streamlines.

A close-up view of Fig. 10 is displayed in Fig. 11 where the effect of cavitation on the thrust force can also be seen. Because of a lower density of the vapor compared to that of the liquid, when cavitation occurs, the shear stresses and as a result, the thrust forces on the valve are decreased. Figure 11 shows that for all poppet angles, this reduction of the thrust force at the cavitation time is occurring. As an example, for the valve with an angle of 45°, the cavitation occurs at 35.6 ms elapsed after the start of the flow into the channel. This time corresponds to a flow rate of 21.35 cm^3/s (see Fig. 6) and, as seen in Fig. 11, the thrust force for this valve angle is slightly decreased at a flow rate of nearly 21cm^3/s.

The average downstream pressure variation against time (or valve inflow) is shown in Fig. 12. For a valve angle of 45°, the pressure becomes negative at the start of the flow because of a sharp diverging shape of the poppet in this case. The pressure then is increased as the flow rate is increased. This pressure oscillation is also visible for other cases. When the valve angle is increased, the wavelength of the oscillation is increased and its magnitude is decreased. For a valve angle of 115°, the magnitude of oscillation is minimum which indicates another reason for this valve to be more favorable.

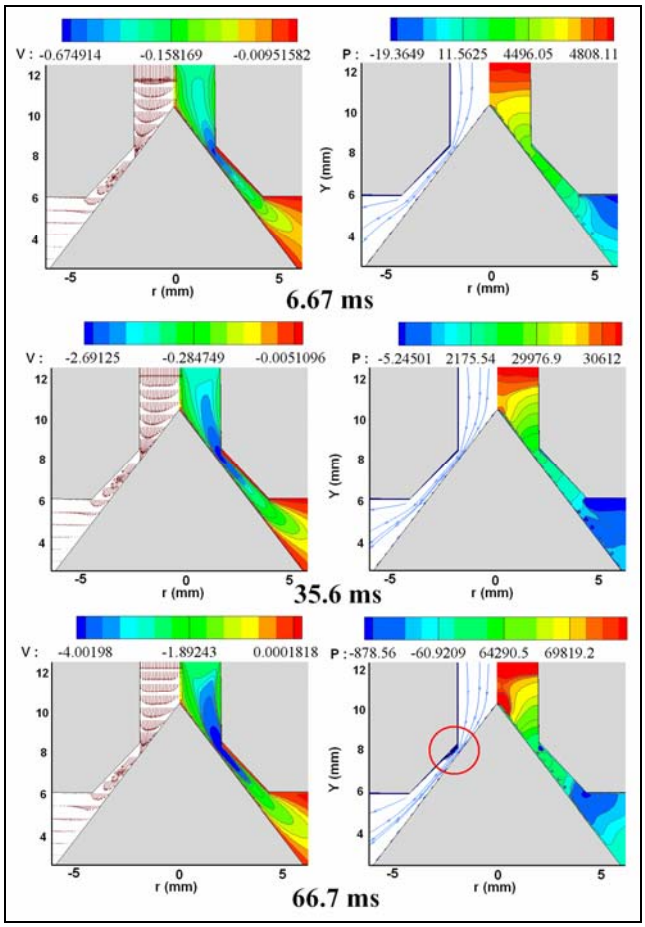

Fig. 7. Cavity formation (shown in a circle) in a poppet valve with 75º angle. Left: velocity distribution and contours. Right: pressure distribution and flow streamlines.

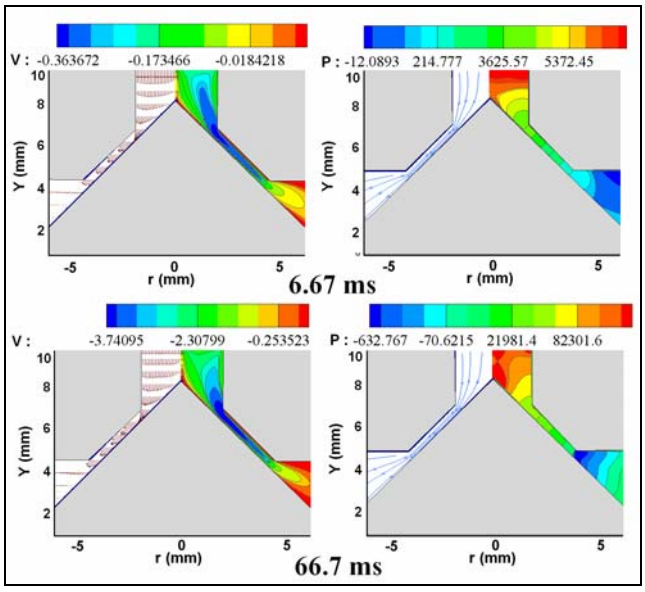

Fig. 8. Flow simulation in a poppet valve with 90º angle. Left: velocity distribution and contours. Right: pressure distribution and flow streamlines. No cavity is formed in this case.

The flow passing ratio (ξ) as an indication of the amount of cavitation is shown in Fig. 13. In this figure, only the cases for which cavitation occurs are displayed. As the valve angle is increased, the time that the flow reaches the cavitation is also increased. Therefore, increasing the poppet angle delays the cavitation time and increases the valve hydraulic efficiency.

Finally, to study the effect of poppet angle on the location of the cavity in a poppet valve operation, the steady inflow rate of 119 cm^3/s is simulated for various poppet angles. The Reynolds number of this flow rate is less than 520 in the valve entrance and around 1200 in the valve minimum cross-sectional area. The results, displayed in Fig. 14, show that for a valve with a smaller poppet angle, the cavity region is more extended through the flow channel. With increasing the angle, the cavity is moved further downstream.

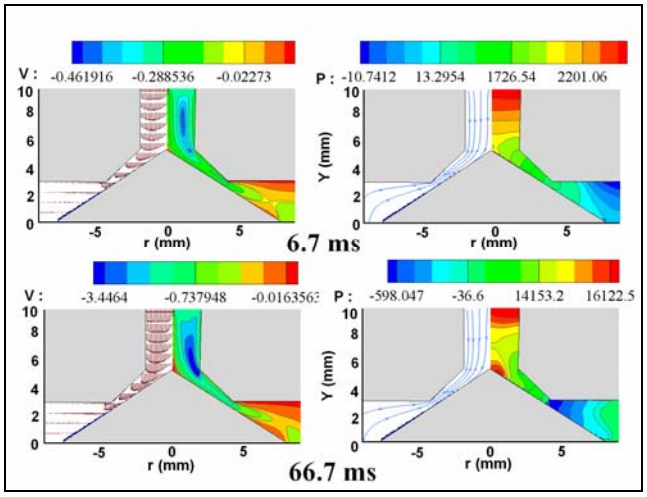

Fig. 9. Flow simulation in a poppet valve with 115º angle. Left: velocity distribution and contours. Right: pressure distribution and flow streamlines. No cavity is formed in this case.

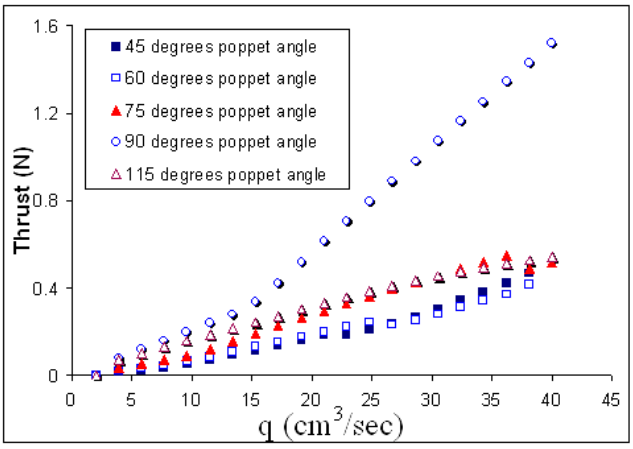

Fig. 10. Thrust force vs. inflow rate for various poppet angles. For all cases, the flow rate was increased from 2 to 40 cm^3/s in 66.7ms.

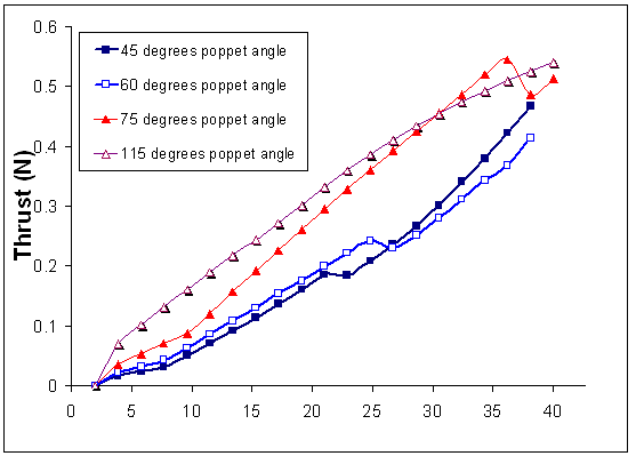

Fig. 11. Close-up view of the thrust force vs. flow rate for 45º, 60º, 75º and 115º poppet angles.

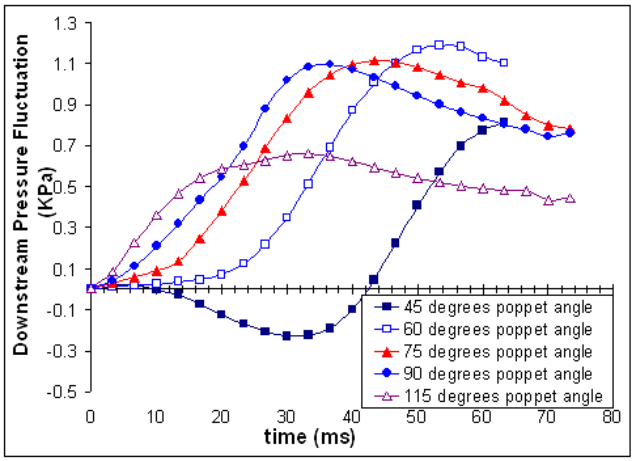

Fig. 12. Downstream pressure fluctuation vs. time for different poppet angles. For all cases, the flow rate was increased from 2 to 40 cm^3/s in 66.7 ms.

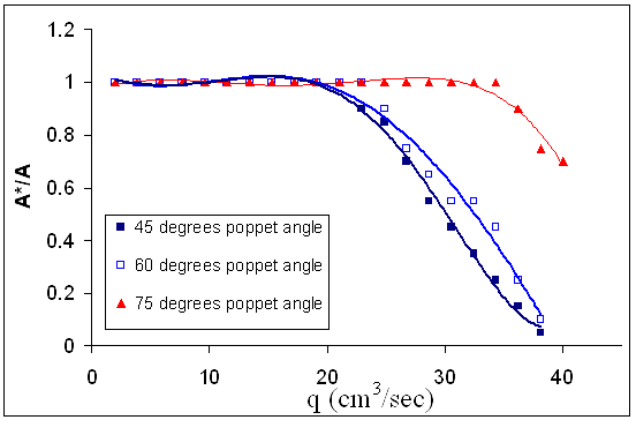

Fig. 13. Flow passing ratio (A^*/A) vs. flow rate for 45º, 60º, and 75º poppet angles. The flow rate was increased from 2 to 40 cm^3/s in 66.7ms.

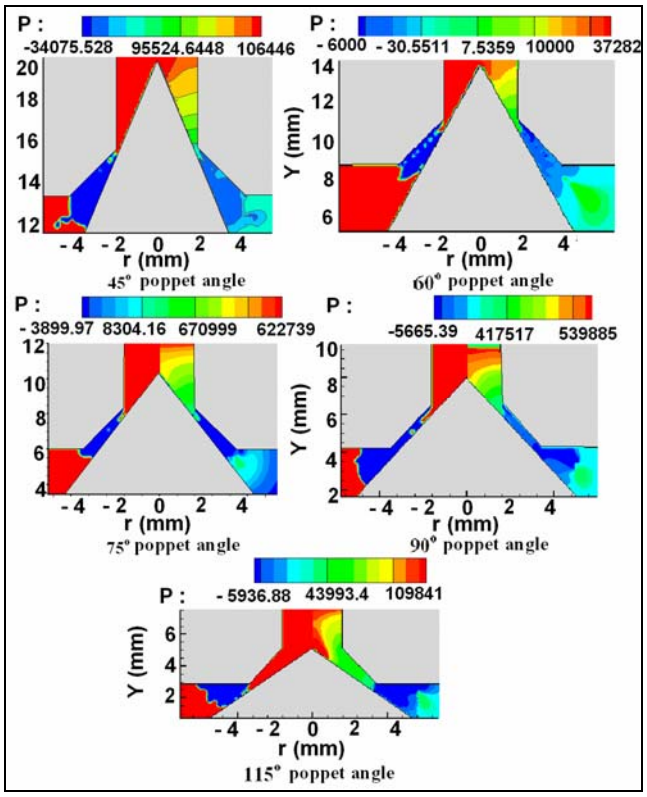

Fig. 14. The effect of poppet angle on the location of the cavity and flow pressure distribution. The flow rate through the valve for all cases was 119 cm^3/s. In each image, the left side of the valve shows the cavity and the right side displays the pressure distribution.

CONCLUSION

In this paper, the cavitation regimes in an oil hydraulic poppet valve are investigated using a computational model. Transient numerical results are well compared with those of the available experiment in the literature. When a cavity is formed at the valve seat, a serious fault occurs in its performance. The model, therefore, can be used as a design tool to investigate the effect of valve geometric parameters on the performance of the valve with regard to cavitation. The effect of poppet angle on the valve performance was also investigated. When the poppet angle is increased the cavitation is delayed. A valve with a poppet angle more than the seat angle was found to be more favorable in terms of eliminating cavitation and reducing pressure fluctuation.

NOMENCLATURE

A	Minimum cross-sectional flow area around poppet (m^2)
A^*	Liquid passing area with no cavitation (m^2)
$\vec{F}_b$	Body force acting on the fluid per unit volume (N/m^3)
$\vec{g}$	Gravitational acceleration (m/s^2)
Min	Minimum
n	Time level
P	Pressure (Pa)
P_D	Downstream pressure (Pa)
P_U	Upstream pressure (Pa)
P_v	Vapor pressure (Pa)
P_∞	Main flow pressure (Pa)
q	Volume flow rate (m^3/s)
S	Mass transfer sink term
t	Time (s)
t_∞	Flow characteristic time (s)
$\vec{V}$	Velocity vector (m/s)
V_∞	Main flow velocity (m/s)
x	Poppet displacement (mm)
μ	Viscosity (Kg/m.s)
θ	Poppet angle (degrees)
ρ	Density (Kg/m^3)
σ	Cavitation number

REFERENCES

Ahuja, V., and Hosangadi, A., 2006, Analysis of Unsteady Cavitation in Rocket Feed Systems and Flow Control Element, in proceeding of Sixth International Symposium on Cavitation (CAV2006), Wageningen, The Netherlands.

Brackbill, J. U., Kothe, D. B. and Zamach, C., 1992, A continuum method for modeling surface tension, *J. Comput. Phys*., Vol. 100, pp. 335-354.

Bussmann, M., Mostaghimi, J., and Chandra, S., 1999, On a Three-Dimensional Volume Tracking Model of Droplet Impact, *J. Phys. Fluid*, Vol. 11, p. 1406.

Dumont, N., Simonion, O., and Habchi, C., 2001, Numerical Simulation of Cavitating Flows in Diesel Injectors by a Homogenous Equilibrium Modeling Approach, In proceeding of 4th International Symposium on Cavitation (CAV2001).

Frobenius, M., and Schilling, R., 2003, Three-dimensional unsteady cavitating effects on a single hydrofoil and in a radial pump-measurement and numerical simulation, in Proceedings of the 5th International Symposium on Cavitation (CAV 2003), Osaka, Japan.

Hirt, F. H. and Nichols, B. D., 1981, A computational method for free surface hydrodynamics, *J. Comput. Phys*., Vol. 39, p. 201.

Kikui, Shotaro., Washio, Seiichi., Takahashi, Satoshi ., 2006, Observation of cavitation in oil hydraulic poppet valve, In proceeding of Sixth International Symposium on Cavitation (CAV2006), Wageningen, The Netherlands.

Kunz, R. F., Boger, D. A., Stinebring, D. R., Chyczewski, T. S., Lindau, J. W., and Gibeling, H. J., 2000, A preconditioned Navier-Stokes method for two-phase flows with application to cavitation, *J. Computers & Fluids*, Vol. 29, pp. 849-875.

Merkle, C. L., Feng, J., and Buelow, P.E.O., 1998, Computational modeling of the dynamics of sheet cavitation, in Proceedings of the 3rd International Symposium on Cavitation, (CAV1998), Grenoble, France.

Passandideh-Fard, M., and Roohi, E., 2008 (in print), Transient Simulations of Cavitating Flows using a Modified Volume-of-Fluid (VOF) Technique, *Int. J. of Comput. Fluid Dynamics*.

Singhal, N. H., Athavale, A. K., Li, M. and Jiang, Y., 2002, Mathematical basis and validation of the full cavitation model, *J. of Fluids Engineering*, Vol. 124, pp. 1-8.

Takahashi, S., Washio, S., Uemura, K., Okazaki, A., 2003, Experimental Study on Cavitation Starting at and Flow Characteristics Close to the Point of Separation, in Proceedings of the 5th International Symposium on Cavitation (CAV 2003), Osaka, Japan.

Wiesche, S., 2005, Numerical simulation of cavitation effects behind obstacles and in an automotive fuel jet pump, *J. Heat Mass Transfer,* Vol. 41, pp. 615-624.

Youngs, D. L., 1982, Time dependent multi material flow with large fluid distortion, *J. Num. Methods for Fluid Dynamics*, N.Y, 273-285.

Yuan, W., Sauer, J., and Schnerr, G. H., 2001, Modeling and computation of unsteady cavitation flows in injection nozzles *J. of Mechanical Ind.*, Vol. 2, pp. 383-394.